Physica A 559 (2020) 125121

Contents lists available at ScienceDirect

Physica A

journal homepage: www.elsevier.com/locate/physa

Transfer entropy calculation for short time sequences with application to stock markets

Lu Qiu [a,b,*], Huijie Yang [c]

[a] School of Finance and Business, Shanghai Normal University, Shanghai 200234, China
[b] Department of Finance, East China University of Science and Technology, Shanghai 200237, China
[c] Business School, University of Shanghai for Science and Technology, Shanghai 200093, China

ARTICLE INFO

Article history:
Received 27 November 2019
Received in revised form 26 July 2020
Available online 21 August 2020

Keywords:
Financial short time series
Transfer entropy
Financial crisis
Early warning

ABSTRACT

We investigate the estimation of transfer entropy (TE) for short time sequences by correlation-dependent balanced estimation of diffusion entropy employed in the transfer entropy (CBEDETE) method and the normal transfer entropy (NTE) method. Our finding shows that the CBEDETE method is more effective than the NTE method on TE calculation for short time series. Based on this conclusion, we use 38 important stock market indices from 4 continents to create successive financial networks with 10∼60-day windows and 1-day step by the CBEDETE method. By extracting the evolution characteristics of out-/in-degree of stock networks, we obtain the most influential stocks RTS, KOSPI, PSI, NIKKE and AORD of Europe, Asia and Oceania and the most influenced stocks IBOVESPA, NYSE, NASD and MERV of America. Finally, by monitoring the ratio of link numbers of each network and smoothing the curves, we find an interesting result that almost all effective peaks in the smoothed ratio curves are prior to the financial crises, such as the global financial crisis in 2008, China's stock market crash in 2015, etc.

1. Introduction

The dynamic complex system has become an important trend in researching the evolution of the financial market [1]. Researchers can get several vital dynamic evolvement properties by monitoring the evolving structures of correlation networks [2–5]. The correlation network can be created by methods including Pearson correlation [6], Granger causality [7,8], mutual information [9] and transfer entropy [10,11]. Correlation networks have become essential tools for researching the financial market, extracting more information about the movement of the stock market, and serving as an indicator of financial crisis and risk management. Pearson correlation and Granger causality are used for linear correlation. By using the Granger causality method, researchers can access the impact of one stock on another one. However, there are some nonlinear correlations among stocks, especially when the linear correlation of two stocks is relatively small, that is, more nonlinear components than linear ones between two stocks. Though the mutual information can be used to determine the strength of nonlinear correlations, it may fail to lend itself to nonlinear causal analysis. By contrast, transfer entropy, which can be used to estimate both the nonlinear and the causal correlation, has been adopted by more investigators.

Researchers often use long sequences to calculate transfer entropy because limited data records may bring unacceptable noise to the final result. Leonidas Sandoval used the 197 largest financial companies in the world, from 2002 to 2012 with length of 2794. They found that Greece, Cyprus, Ireland, Spain, Portugal, and Italy suffered most from the global

* Corresponding author at: School of Finance and Business, Shanghai Normal University, Shanghai 200234, China.
E-mail address: nuaaqiulu@shnu.edu.cn (L. Qiu).

https://doi.org/10.1016/j.physa.2020.125121
0378-4371/

credit crisis [12]. Okyu Kwon et al. used 25 stock indices from the period 2000∼2007 (about 1800 points) to calculate the TE of each two stocks, by utilizing the minimum spanning tree (MST) method to construct complex networks. These static directed networks can reveal causality relations between nodes [13]. He et al. analyzed the relationships between 9 stocks from the U.S., Europe and China (from 1995 to 2015, about 4500 points) by using NTE (normal transfer entropy) method. The results showed that the U.S. took the leading position in lagged-current cases and China was the most influential when it comes to same-day indices [14]. Mao et al. added the time-delay embedding theory to the calculation of transfer entropy for high dimensional series and analyzed the information flow between different stocks from 2011 to 2015 (about 1000 points) [15]. Zhou et al. calculated the transfer entropy based on 10 stock market in the period from January 1992 to March 2017 (a total of 5040 records) and successively moved a 12-month window by 1-month steps to find indicators of financial crisis [16]. Mario et al. calculated symbolic transfer entropy by using 120 different assets in the BME Spanish stock exchange from 01/01/2000 until 12/31/2008 (1969 trading days) and identified relationships between financial traders [17].

The above researchers often use several long series (covered about $10^3 \sim 10^4$ points) to create static networks to describe the topology of financial market. However, the state network evolution of stock markets can hardly be discovered by static networks. To avoid this, researchers often calculate the topologies of successive financial networks (2∼ 6-month-window and 1∼ 2-month-step). Buccheri et al. used 49 industry index time series whose time period ranged from July 1969 to December 2011, spanning more than 40 years, using 3 months as the time scale with a 1-month step. By investigating the average Pearson correlation structure dynamics monthly, they mapped the peaks in the figure of correlation structure evolution onto many vital financial crises such as the Asian crisis in 1997 and global financial crisis in 2008[18]. Munnix et al. used the k-means clustering method to group the moving correlation structure into 8 categories. The number of the categories was used to replace the correlation structure in the figure of temporal evolution (3 months)of the market state. By using the number of states, financial crises such as the 2008∼2009 credit crunch and the 2002 "dot-com bubble" were mapped [19]. Qiu et al. cut the DJI stocks from 1992 to 2013 into 241 parts with the 2-month window and 1-month step. They created financial state networks by using the planer maximally filtered graph (PMFG) method and found that the financial crisis states were in the same community [20]. Kang et al. analyzed the dynamic volatility spillovers and network connectedness between stock indexes. With 200-day rolling windows, they found the highest level of spillover index during the 2008∼2009 global financial crisis and the 2010∼2012 European sovereign debt crisis [21]. Due to the accuracy of correlation calculation of short series, the above researchers used 2∼6 months as the window size. The corresponding networks indicating correlations of stocks of even half a year affect the accuracy of early warning of financial crisis [22].

According to the above research, there are two problems in need of further investigation. The first one is how to decrease the bias when calculating the TE between short series. The other one is how to find the indicator of financial crisis from dynamic financial networks. In this letter, we seek to address the above two problems. We use the correlation-dependent balanced estimation of diffusion entropy (CBEDE) method [23,24] to decrease the deviation when calculating the TE between short series, a practice known as CBEDETE. On the basis of accurate estimations of the TE between short series, we use 38 stock indices from different markets to create successive financial networks and extract characteristics from the networks as indicators of financial crises.

The rest of the paper is organized as follows. In Section 2, we briefly introduce the fundamental implication of TE and present a review of balanced estimation of diffusion entropy (BEDE) [25,26] and CBEDE. We also contrast TE calculation with the CBEDETE method and with the NTE method. In Section 3, we show the main results: one is the comparison between CBEDETE and NTE; the other is the application the CBEDETE method to the impact of financial crisis and crisis early warning. Section 4 is our conclusion and discussion.

2. Methodologies

2.1. Normal method for estimation of transfer entropy

Transfer entropy was developed by Schreiber. It is a measure to evaluate dynamic, nonlinear, and non-symmetric relationships [15]. The definition of Shannon Entropy is as follows:

$$H = -\sum_{i=1}^{M} p_i \log p_i, \tag{1}$$

for a sequence x and $p_i \neq 0$, where M is the number of bins by dividing the sequence x, p_i is the probability of the ith bin by probability density function (PDF). Based on Shannon entropy, transfer entropy can be conceived as a parameter which can be used for describing the interaction between series X and Y. The reciprocities have directivity, $TE_{x\to y}$ or $TE_{y\to x}$. The transition probabilities can be defined as follows:

$$p(x_{i+1} \mid x_i^{(k)}, y_i^{(l)}) = p(X_{i+1} = x_{i+1} \mid X_i^{(k)} = x_i^{(k)}, Y_i^{(l)} = y_i^{(l)}) \tag{2}$$

Table 1
The combined events. From $p1$ to $p8$ respectively represent 8 probability events of two-bins condition, sum from $p1$ to $p8$ is 1.

A	B	C	pi
0	0	0	p1
0	0	1	p2
0	1	0	p3
0	1	1	p4
1	0	0	p5
1	0	1	p6
1	1	0	p7
1	1	1	p8

where time series of X could be treated as a Markov process of degree k. Likewise, Y is j degree Markov process. $X_i^{(k)} = (X_i, X_{i-1}, \ldots, X_{i-k+1})$ and $Y_i^{(l)} = (Y_i, Y_{i-1}, \ldots, Y_{i-l+1})$. $x_i^{(k)}$ and $y_i^{(k)}$ are the states of $X_i^{(k)}$ and $Y_i^{(l)}$ respectively. The transfer entropy from a variable Y to the other variable X is defined as follows:

$$\begin{aligned} &TE_{Y\to X}(k,l) \\ &= H(X_{i+1} \mid X_i^{(k)}) - H(X_{i+1} \mid X_i^{(k)}, Y_i^{(l)}) \\ &= \sum p(x_{i+1}, x_i^{(k)}, y_i^{(l)}) \log \frac{p(x_{i+1} \mid x_i^{(k)}, y_i^{(l)})}{p(x_{i+1} \mid x_i^{(k)})} \\ &= \sum_{i_{n+1}, i_n^{(k)}, j_n^{(l)}} p(i_{n+1}, i_n^{(k)}, j_n^{(l)}) \log \frac{p(i_{n+1}, i_n^{(k)}, j_n^{(l)}) p(i_n^{(k)})}{p(i_{n+1}, i_n^{(l)}) p(i_n^{(k)}, j_n^{(l)})} \end{aligned} \tag{3}$$

where i_n is element n of the time series of variable X and j_n is element n of the time series of variable Y. To facilitate the calculation of transfer entropy, we take $k = l = 1$. Thus the normal formula for transfer entropy of Y to X is as follows:

$$NTE_{Y\to X} = \sum_{i_{n+1}, i_n, j_n} p(i_{n+1}, i_n, j_n) log \frac{p(i_{n+1}, i_n, j_n) p(i_n)}{p(i_{n+1}, i_n) p(i_n, j_n)} \tag{4}$$

For easy calculating based on Eq. (4), we let A replace i_{n+1}, B, i_n, C, j_n. For example, if $X = [0.5, 0.6, 0.55, 0.7, 0.4, 0.3, 0.4, 0.1, 0.57, 0.46, 0.5]$, $Y = [0.3, 0.4, 0.5, 0.4, 0.7, 0.8, 0.45, 0.44, 0.5, 0.2, 0.7]$, we take 10-length segment as a research section. The corresponding objects are $A = [0.6, 0.55, 0.7, 0.4, 0.3, 0.4, 0.1, 0.57, 0.46, 0.5]$, $B = [0.5, 0.6, 0.55, 0.7, 0.4, 0.3, 0.4, 0.1, 0.57, 0.46]$, and $C = [0.3, 0.4, 0.5, 0.4, 0.7, 0.8, 0.45, 0.44, 0.5, 0.2]$. The formula of transfer entropy can be rewritten as follows:

$$\begin{aligned} TE_{Y\to X} &= \sum p(ABC) \log \frac{p(ABC)p(B)}{p(AB)p(BC)} \\ &= \sum p(ABC) \log p(ABC) + \sum p(B) \log p(B) \\ &\quad - \sum p(AB) \log p(AB) - \sum p(BC) \log p(BC) \end{aligned} \tag{5}$$

In formula (5), assuming that there are only two dividing sections for all sequences indicating 0 and 1 respectively, we define these variables as 2 bins shown in Table 1, where 8 events (e1, e2, …, e8) whose sum of probabilistic combination ($p1, p2, \ldots, p8$) equals one. The corresponding sample of probabilistic combination is shown in Fig. 1. For two split sections, there are 8 events. When the split section equals $3(3^3 = 27\ events)$, $4(4^3 = 64\ events)$ *and* $5(5^3 = 125\ events)$, the number of events increase exponentially over time. For a short time series, each point corresponds to an event. When the length of time series equals 10 or 20, some events are unavailable because the number of events exceeds the length of time series ($\{27, 64, 125\} > \{10, 20\}$). The accuracy of TE calculation will be impacted by non-matched events.

2.2. Correlation-dependent balanced estimation of diffusion entropy

In order to revise the bias of transition entropy calculation in short sequences, we use the CBEDE method to calculate the transfer entropy which is named CBEDETE.

Prior to the CBEDETE calculation, let us consider a stationary time series, $\xi_1, \xi_2, \ldots, \xi_L$. All the possible segments with length s read,

$$X_i = \{\xi_i, \xi_{i+1}, \ldots, \xi_{i+s-1}\}, i = 1, 2, \ldots, N - s + 1. \tag{6}$$

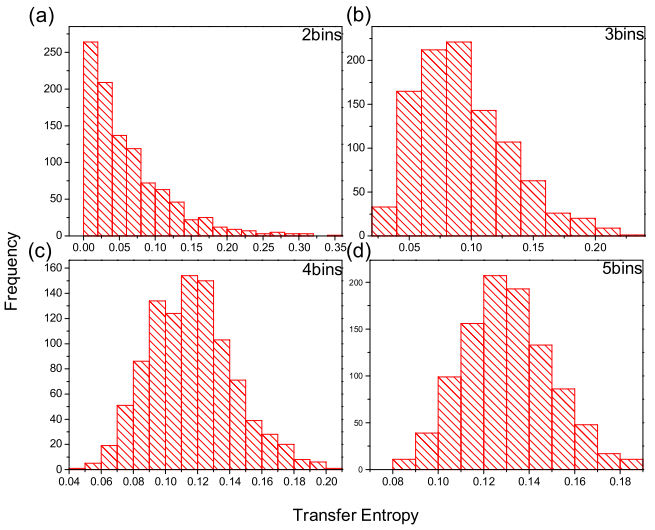

Fig. 1. The theoretical transfer entropy distribution. (a), (b), (c) and (d) indicate the distributions of theoretical transfer entropy from 2 bins to 5 bins.

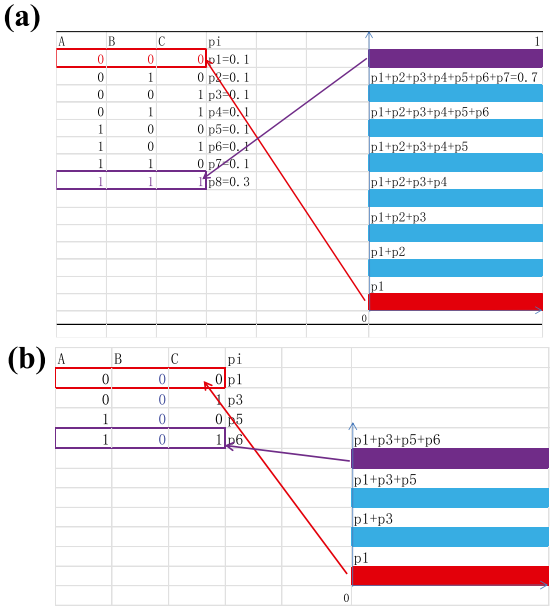

Fig. 2. The rules of event selection. (a) The first step for choice of event group. The red region corresponds to the first event group [0,0,0], the blue regions the second to the seventh event groups, the violet region the eighth event group [1,1,1]. (b) The second step for choice of event group. The red region corresponds to the first event group [0,0,0], the blue regions the second and third event groups, the violet region the fourth event group [1,0,1]. With the assumption that $p1 = 0.1, p2 = 0.1, p3 = 0.1, p4 = 0.1, p5 = 0.1, p6 = 0.1, p7 = 0.1, p8 = 0.3$, we define the probabilistic interval $[0, p1]$, in the red region of (a) as the probability of the event indicating $A = 0, B = 0, C = 0$. Similarly, the purple region in (a) corresponding to $A = 1, B = 1, C = 1$ matches with the probabilistic interval $(0.7, 1]$. For example, if we generate a random number 0.45 in the interval $(0.4, 0.5]$, then the choice of the event is $A = 1, B = 0, C = 0$.

now we regard X_i as a realization of a stochastic process, namely, a trajectory of a particle starting from the original point and the duration time is a total of s time units. All the $N - s + 1$ trajectories form an ensemble, whose displacements, $x(s) = \{x_1(s), x_2(s), \ldots, x_{N-s+1}(s)\}$, are

$$x_i(s) = \sum_{j=1}^{s} \xi_j, i = 1, 2, \ldots, N - s + 1. \tag{7}$$

A(i_{n+1})	B(i_n)	C(j_n)
0	1	1
1	0	0
0	1	1
0	0	0
0	0	0
0	0	0
1	0	0
0	1	1
0	0	0
0	0	1

Fig. 3. A sample of one-group event. The yellow region means $A_1 = B_2$, and the blue region indicates $A_2 = B_3$. The last pair indicates $A_9 = B_{10}$ shown by violet region.

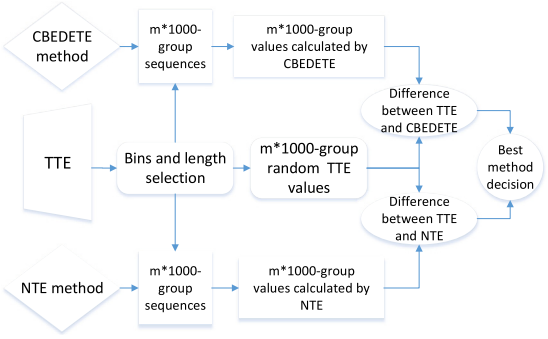

Fig. 4. The flowchart of comparison between CBEDETE and NTE.

dividing the distribution region of displacement into $M(s)$ bins, the PDF can be naively approximated as,

$$p(k,s) \sim \hat{p}(k,s) = \frac{n(k,s)}{N - M(s) + 1}, k = 1, 2, \ldots, M(s), \tag{8}$$

where $n(k,s)$ is the number of displacements occurring in the kth bin. The consequent naive estimation of diffusion entropy of the process reads,

$$S_{DE}(s) \sim S_{DE}^{naive}(s) = -\sum_{j=1}^{M(s)} \hat{p}(j,s) \ln[\hat{p}(j,s)]. \tag{9}$$

We assume the time series abides by scale-invariance, namely, $p(j,s)$ satisfies,

$$\begin{aligned} \hat{p}(j,s) &= \frac{1}{s^\delta} F\left(\frac{min[x(s)] + (j-0.5)\epsilon(s)}{s^\delta}\right) \times \epsilon(s) \\ &\equiv \frac{1}{s^\delta} F\left(\frac{x_j^c}{s^\delta}\right) \times \epsilon(s) \\ j &= 1, 2, \ldots, M(s), \end{aligned} \tag{10}$$

where $\epsilon(s)$ is the window size, and $x_j^c \equiv min[x(s)] + (j-0.5)\epsilon(s)$, i.e., the central point of the jth bin. Formula (9) can be rewritten as,

$$S_{DE}^{naive}(s) = -\sum_{j=1}^{M(s)} \frac{\epsilon(s)}{s^\delta} F\left(\frac{x_j^c(s)}{s^\delta}\right) \left[ln\epsilon(s) + lnF\left(\frac{x_j^c}{s^\delta}\right) - \delta lns\right]. \tag{11}$$

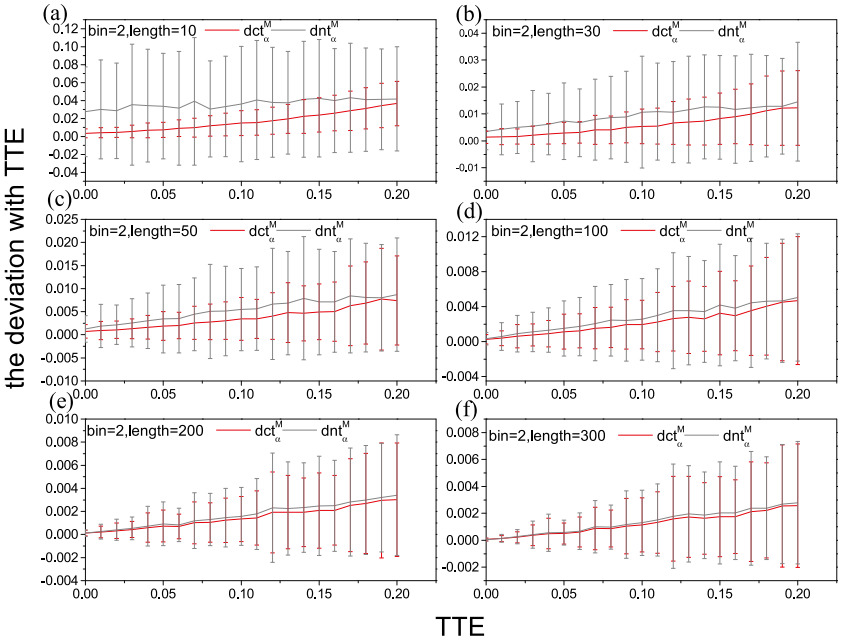

Fig. 5. The deviation of CBEDETE method and NTE method in the 2-bin condition. The horizontal axis means the theoretical transfer entropy. The vertical axis represents the differences (indicated by red lines) between CBEDETE and TTE, and the differences (indicated by blue lines) between NTE and TTE.

If the length of the time series is infinite, i.e., $N \to \infty$ and $\frac{\epsilon(s)}{s^\delta} \to d(\frac{x_j^c(s)}{s^\delta})$, the naive estimation of entropy can be approximated with a integral form, which reads,

$$\begin{aligned} S_{DE}^{naive}(s) &= -\int_{min[x(s)]}^{max[x(s)]} d\left(\frac{x}{s^\delta}\right) F\left(\frac{x}{s^\delta}\right) \times \left[lnF\left(\frac{x}{s^\delta}\right) - \delta lns\right] \\ &= -\int_{min[x(s)]}^{max[x(s)]} dyF(y) \times [lnF(y) - \delta lns] \\ &= A + \delta lns, \end{aligned} \tag{12}$$

where $A = -\int_{min[x(s)]}^{max[x(s)]} dyF(y)lnF(y)$, a constant.

Hence, the simple relation of Formula (12) can be used to detect scalings in time series. It is the first tool yielding correct scalings in both the Gaussian and the Lévy statistics. For this reason, it is used to detect scale-invariance in diverse research fields [27], such as solar activities[28,29], spectra of complex networks [30], physiological signals [31], and finance [32].

In the DE method, the bin size $\epsilon(s)$ is generally chosen to be a certain fraction of the standard deviation of the considered time series. With the increase of s, both the characteristic distribution width of $x(s)$ (i.e., standard deviation of $x(s)$) and the number of bins $M(s)$ will increase rapidly according to s^δ. For finite N, the naive estimation of relative frequencies may lead to large fluctuations and bias to the calculations in downstream steps. Defining an error variable, $\mu(j,s) = \frac{\hat{p}(j,s)-p(j,s)}{p(j,s)}$, a straightforward computation leads to a rough estimation of bias, $S_{DE}^{bias}(s) \equiv S_{DE}(s) - S_{DE}^{naive} = \frac{M(s)-1}{2(N-s+1)} + O(M(s))$. Consequently, $S_{DE}^{naive}(s)$ deviates significantly from the true entropy not only statistically but also systematically.

Our goal is to find a proper estimation of diffusion entropy to reduce simultaneously the bias and the variance as much as possible, which can be formulated as an optimal problem. For simplicity, the variable s is not written explicitly in the following formulas. Let us denote the occurring probabilities and realization numbers in the M bins with $\vec{p} = (p_1, p_2, \ldots, p_M)$, and $\vec{n} = (n_1, n_2, \ldots, n_M)$, respectively. One can define bias and statistical fluctuation as,

$$\begin{aligned} \Delta_{bias}^2 &\equiv \left(\langle\hat{S}\rangle - S\right)^2, \\ \Delta_{stat}^2 &\equiv \left\langle\left(\hat{S} - \langle\hat{S}\rangle\right)^2\right\rangle, \end{aligned} \tag{13}$$

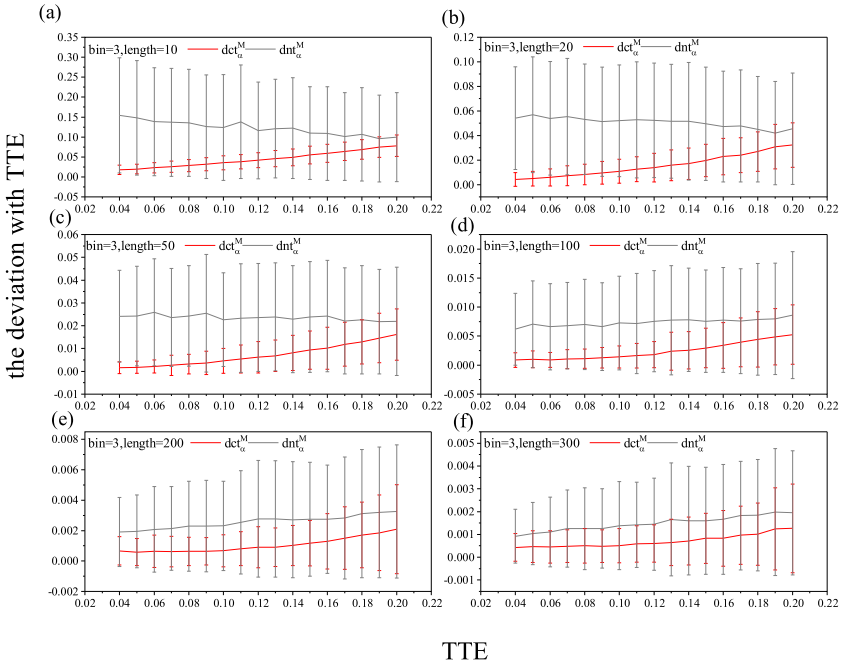

Fig. 6. The deviation of CBEDETE method and NTE method in the 3-bin condition. The horizontal axis means the theoretical transfer entropy. The vertical axis represents the differences (indicated by red lines) between CBEDETE and TTE, and the differences (indicated by blue lines) between NTE and TTE.

where $\hat{S}$ is the estimation of real diffusion entropy $S \equiv -\vec{p} \cdot ln\vec{p}$, and $\langle\cdot\rangle$ the average over all possible configurations of $\vec{n}$. To balance the errors, we consider the total error averaged over all the configurations of $\vec{p}$, which reads,

$$\begin{aligned}\Delta^2 &= \int_{\sum_{i=1}^{M} p_i=1} d\vec{p} \cdot [\Delta^2_{bias} + \Delta^2_{stat}] \\ &= \int_{\sum_{i=1}^{M} p_i=1} d\vec{p} \cdot \left\{ \sum_{\sum_{j=1}^{M} n_j=N-s+1} P(\vec{n},\vec{p}) \cdot \hat{S}^2(\vec{n}) + S^2(\vec{p}) \right\} \\ &- \int_{\sum_{i=1}^{M} p_i=1} d\vec{p} \left\{ 2S(\vec{p}) \cdot \left[\sum_{\sum_{j=1}^{M} n_j=N-s+1} P(\vec{n},\vec{p})\hat{S}(\vec{n}) \right] \right\}\end{aligned} \tag{14}$$

where $P(\vec{n},\vec{p})$ is the binomial distribution,

$$P(\vec{n},\vec{p}) = \frac{\left(\sum_{i=1}^{M} n_i\right)! \prod_{i=1}^{M} p_i^{n_i}}{\prod_{i=1}^{M} n_i!}. \tag{15}$$

The expected values of $\hat{S}(\vec{n})$ should lead to the minima of the averaged error, which requires a necessary condition:

$$\begin{aligned}&\frac{\partial \Delta^2}{\partial \hat{S}(\vec{n})} = 2 \int_{\sum_{i=1}^{M} p_i=1} d\vec{p} P(\vec{p},\vec{n}) \hat{S}(\vec{n}) \\ &- 2 \int_{\sum_{i=1}^{M} p_i=1} d\vec{p} P(\vec{p},\vec{n}) S(\vec{p}) = 0\end{aligned} \tag{16}$$

for all the possible configurations of $\vec{n}$. A simple transformation leads to,

$$\begin{aligned}\hat{S}(\vec{n}) &= \frac{\int_{\sum_{i=1}^{M} p_i=1} d\vec{p} \cdot S(\vec{p}) \cdot P(\vec{n},\vec{p})}{\int_{\sum_{i=1}^{M} p_i=1} d\vec{p} P(\vec{n},\vec{p})} \\ &= \frac{-\sum_{j=1}^{M} \lim_{z\to 1} \left[\int_{\sum_{i=1}^{M} p_i=1} d\vec{p} \cdot p_j^z \cdot P(\vec{n},\vec{p}) \right]'_z}{\int_{\sum_{i=1}^{M} p_i=1} d\vec{p} P(\vec{n},\vec{p})},\end{aligned} \tag{17}$$

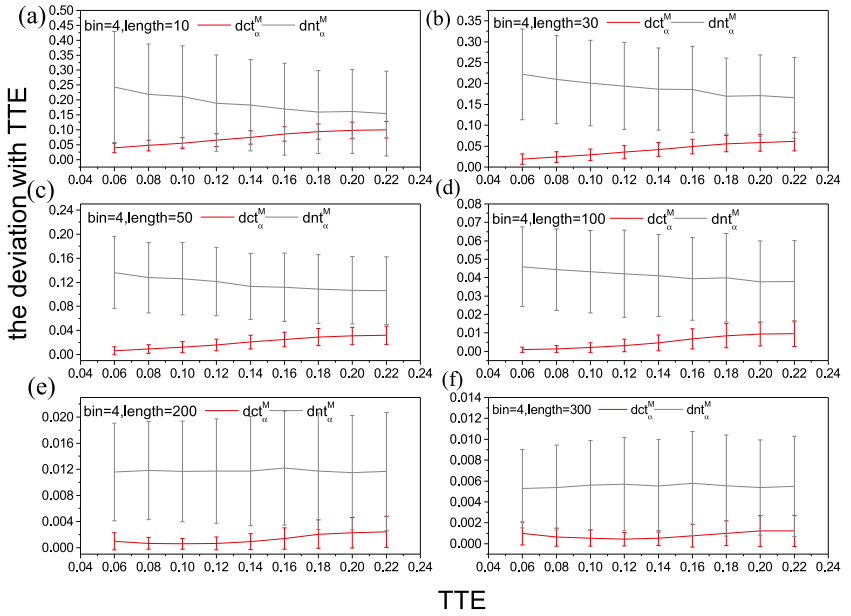

Fig. 7. The deviation of CBEDETE method and NTE method in the 4-bin condition. The horizontal axis means the theoretical transfer entropy. The vertical axis represents the differences (indicated by red lines) between CBEDETE and TTE, and the differences (indicated by blue lines) between NTE and TTE.

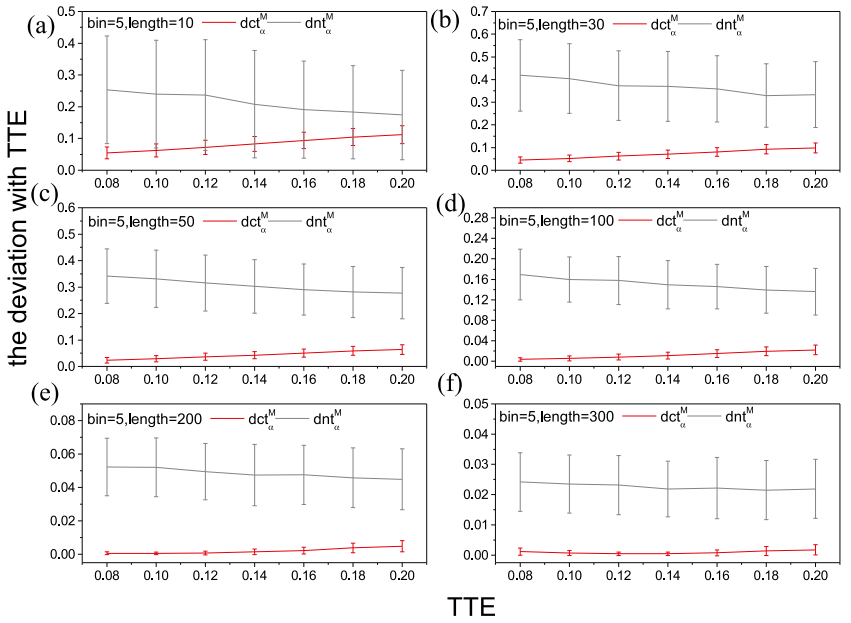

Fig. 8. The deviation of CBEDETE method and NTE method in the 5-bin condition. The horizontal axis means the theoretical transfer entropy. The vertical axis represents the differences (indicated by red lines) between CBEDETE and TTE, and the differences (indicated by blue lines) between NTE and TTE.

where we use the identity, $p_j lnp_j \equiv \lim_{z\to 1} \frac{dp_j^z}{dz}$. The final estimation of diffusion entropy, which reads,

$$\hat{S}_{DE} = \frac{1}{N+M} \sum_{j=1}^{M} (n_j + 1) \sum_{k=n_j+2}^{N+M} \frac{1}{k} \tag{18}$$

If the diffusion process is considered, the expression formula is as follows [23,24]:

$$\hat{S}(\vec{n}, s) = \frac{1}{N - s + 1 + M(s)} \sum_{j=1}^{M(s)} [n_j(s) + 1] \cdot \sum_{k=n_j(s)+2}^{N-s+1+M(s)} \frac{1}{k}, \tag{19}$$

which is called correlation-dependent balanced estimation of diffusion entropy (CBEDE). One can find that for the specific case of $M(s) = 2$, CBEDE degenerates to the BEDE. In the actual estimation of transfer entropy, we use formula (18) to calculate each part of formula (5). The calculation formula is as follows,

$$\begin{aligned} CBEDETE_{Y\to X} &= S_{DE}^{ABC} + S_{DE}^{B} - S_{DE}^{AB} - S_{DE}^{BC} \\ &= \frac{1}{N + M_{ABC}} \sum_{j=1}^{M_{ABC}} (n_j^{ABC} + 1) \sum_{k=n_j^{ABC}+2}^{N+M_{ABC}} \frac{1}{k} \\ &+ \frac{1}{N + M_B} \sum_{j=1}^{M_B} (n_j^{B} + 1) \sum_{k=n_j^{B}+2}^{N+M_B} \frac{1}{k} \\ &- \frac{1}{N + M_{AB}} \sum_{j=1}^{M_{AB}} (n_j^{AB} + 1) \sum_{k=n_j^{AB}+2}^{N+M_{AB}} \frac{1}{k} \\ &- \frac{1}{N + M_{BC}} \sum_{j=1}^{M_{BC}} (n_j^{BC} + 1) \sum_{k=n_j^{BC}+2}^{N+M_{BC}} \frac{1}{k} \end{aligned} \tag{20}$$

where N is the length of a segment (X or Y), M is the number of bins divided by the time series. Specifically, $M_{ABC} = M_A * M_B * M_C$ ($M_A = M_B = M_C$). Because of the increase of computational complexity according to number of bins, the number of bins is often set to $2 \sim 5$, expressed as, $M_A = M_B = M_C \subseteq \{2, 3, 4, 5\}$.

2.3. Comparison between NTE and CBEDETE

To compare the two methods (NTE and CBEDETE) for the estimation of transfer entropy, we create the TTE (theoretical value of transfer entropy) by given probability combinations and compare the assessment results from three kinds of assessment methods (NTE, CBEDETE and TTE).

Specifically, we create 1000-group probability combinations. There are 8 values in each group, $p1$, $p2$, $p3$, $p4$, $p5$, $p6$, $p7$, *and*$p8$, such as elements in Table 1. The summation from $p1$ to $p8$ is 1. In order to define a probable range of true transfer entropy with 2 bins, we calculate 1000-group transfer entropies with the 1000-group *pi*s by formula (5). The distribution of TTE is shown in Fig. 1. About all TTEs are in [0, 0.2]. So we choose 19 values with the step being 0.01 in the gap [0, 0.2]. The 19 corresponding group probability combinations are used to calculate the CBEDETE and NTE. The detailed processes for comparing three kinds of TE calculation are as follows:

1. The choice of number of bins. It is important to note that when the number of bins is larger than 5, the computation velocities of CBEDETE and NTE are all much slow. Therefore we only choose 2∼5 bins as examples.

2. The choice of the TTE gap for each bin. As shown in Fig. 1, we choose the main distribution from each of the bins. To be specific, in Fig. 1(a), the corresponding gap is [0 : 0.01 : 0.2]. The other three gaps are [0.4 : 0.01 : 0.2], [0.06 : 0.02 : 0.220] and [0.08 : 0.22] derived from Fig. 1(b), (c) and (d) respectively. It should be noted that the interval of the gap is set to 0.02 in $4 - bin$ and $5 - bin$ conditions to increase the rate of probability combination searching.

Let us take the two bins condition as an example. We repeatedly choose 19 values for TTE in [0, 0.2] with the step of 0.01 for 1000 times, and get 1000-group values calculated by TTE named TTE_{1000} (each group containing 19 values). Each value from the 19 * 1000 groups is calculated by a probability combination constructed by 8 elements ($p1, p2, \ldots, p8$) whose summation is 1 shown in Fig. 2(a). As an example, the length of sequences A,B and C equals 10. Each events-combination follows the standard in Fig. 2(a). When generating a random number (0.486) to calculate TE by the TTE method, the corresponding probability combination is as follows,

$$\begin{Bmatrix} p1 = 0.239 & p2 = 0.014 & p3 = 0.197 & p4 = 0.135 \\ p5 = 0.237 & p6 = 0.106 & p7 = 0.008 & p8 = 0.064 \end{Bmatrix} \tag{21}$$

according to Fig. 2(a), $p1 + p2 + p3 = 0.450 < 0.486 < p1 + p2 + p3 + p4 = 0.585$, so the first event-combination is (0, 1, 1). Because of the sequence requirements of transfer entropy, the second event-combination is $(*, 0, *)$. That means $A_1 = B_2$. The rest probability group of the second event-combination is $p1 + p3 + p5 + p6 = 0.566$. Then we generate a random number equaling 0.343 whose interval range is $p1 + p3 = 0.337 < 0.343 < p1 + p3 + p5 = 0.359$. The second event-combination is set to (1, 0, 0) on the basis of Fig. 2(b). In the same way, we can get the 10 event-combinations shown in Fig. 3.

Table 2
The stock index list.

Continent	Abbreviation of stock index	Country
Asia	KOSPI	Korea
	PSI	Philippine
	JKSE	Indonesia
	STI	Singapore
	Sensex30	India
	FKLI	Malaysia
	TA100	Israel
	Nikkei225	Japan
	TWII	Taiwan, China
	HIS	Hong Kong, China
	HSCEI	Hong Kong, China
	CSI 300	China mainland
	SZI	China mainland
	SSE180	China mainland
	SHI	China mainland
Europe	RTS	Russia
	NZ50	New Zealand
	SSMI	Switzerland
	OMXSPI	Sweden
	OSEAX	Norway
	AEX	Netherlands
	BFX	Belgium
	ATX	Austria
	MIB	Italy
	SMSI	Spain
	DAX	Germany
	CAC40	France
	FTSE100	United Kingdom
America	MERV	Argentina
	IBOVESPA	Brazil
	MXX	Mexico
	TSX	Canada
	AMEX	USA
	NYSE	USA
	NASD	USA
	SPX500	USA
	DJI	USA
Oceania	AORD	Australia

3. By using formula (5) and (20), we calculate the transfer entropy by NTE and CBEDETE with 19 * 1000-group probability combinations, and get 19 * 1000-group values by NTE named NTE_{1000} and 19 * 1000-group values by CBEDETE named $CBEDETE_{1000}$.

4. We calculate the distinction between $CBEDETE_{1000}$ and TTE_{1000}, NTE_{1000} and TTE_{1000}, the concrete forms are shown in formula (22) and (23),

$$dct_{\alpha}^{M} = \frac{1}{1000}\sum_{\beta=1}^{1000}(CBEDETE_{\alpha,\beta}^{M} - TTE_{\alpha,\beta}^{M})^{2} \tag{22}$$

$$dnt_{\alpha}^{M} = \frac{1}{1000}\sum_{\beta=1}^{1000}(NTE_{\alpha,\beta}^{M} - TTE_{\alpha,\beta}^{M})^{2} \tag{23}$$

where dct_{α}^{M} means the difference between CBEDETE and TTE, dnt_{α}^{M} means the difference between NTE and TTE. α indicates the number divided from the gap of TTE, and M is the bin number. Taking two bins as an example ($M = 2$). $\alpha = 1, 2, 3, \ldots, 19$, $\alpha = 1$, $\alpha = 2$ and $\alpha = 19$ indicate the interval (0,0.01], [0,0.01] and [0.19,0.2] respectively. The main program flow chart for comparing the TTE, NTE and CBEDE is shown in Fig. 4.

3. Result

After a series of preparations, in this section we show the result of comparison between the NTE and CBEDETE methods for the TE calculation. We also conduct empirical studies based on world stock markets by using the best method from NTE and CBEDETE.

Table 3
Basic statistics of transfer entropy networks of 1-month sliding window.

Abb.	Market	Out-degree			In-degree			Harmonic centrality		
		Mean	SD	Max	Mean	SD	Max	Mean	SD	Max
KOSPI	Korea	6.96	7.95	32	2.76	3.51	25	14.44	10.89	35
PSI	Philippine	7.75	8.00	37	2.94	3.41	25	14.93	10.37	37
JKSE	Indonesia	5.83	6.81	32	3.17	3.53	18	14.22	9.96	35.5
STI	Singapore	4.49	6.38	30	2.68	3.65	25	12.20	10.96	34.5
Sensex30	India	5.21	6.26	33	3.51	4.18	29	13.79	10.33	35
FKLI	Malaysia	2.25	4.91	29	1.29	3.10	21	6.68	10.19	34
TA100	Israel	4.20	6.08	33	4.76	6.26	36	13.21	11.45	36.5
Nikkei225	Japan	5.32	5.83	33	3.41	3.48	19	15.06	9.19	35
TWII	Taiwan, China	2.97	4.76	30	2.68	3.65	28	11.72	9.94	35
HIS	Hong Kong, China	3.93	4.86	25	3.57	3.76	25	14.71	8.68	33
HSCEI	Hong Kong, China	4.62	4.87	25	4.37	3.83	25	15.96	7.73	33
CSI 300	China mainland	3.06	4.14	23	3.85	3.66	21	14.33	8.12	31.5
SZI	China mainland	3.32	4.03	26	4.32	3.82	22	14.98	7.56	33
SSE180	China mainland	2.77	3.70	25	3.69	3.63	21	13.99	8.09	32.5
SHI	China mainland	2.74	3.88	21	3.52	3.58	21	13.57	8.44	31.5
RTS	Russia	11.02	7.88	34	4.91	3.95	22	18.54	8.81	35
NZ50	New Zealand	2.80	6.15	32	0.95	2.30	21	6.56	10.48	34.5
SSMI	Switzerland	3.22	4.90	25	3.11	3.97	25	12.08	10.48	32
OMXSPI	Sweden	3.36	4.49	25	3.83	4.21	23	13.52	9.96	33
OSEAX	Norway	3.63	4.65	30	3.91	4.23	26	14.14	9.43	35.5
AEX	Netherlands	3.20	4.34	24	3.82	4.10	22	13.44	9.88	32.5
BFX	Belgium	2.60	3.97	25	3.57	4.15	24	12.29	10.20	33
ATX	Austria	4.28	4.87	30	4.56	4.55	27	15.03	9.31	34
MIB	Italy	3.89	4.71	30	4.82	4.20	28	15.26	8.71	32.5
SMSI	Spain	3.47	4.30	27	4.36	4.20	24	14.52	9.05	31
DAX	Germany	2.79	3.50	22	4.39	4.21	26	14.24	9.03	33.5
CAC40	France	2.91	3.85	22	4.08	3.97	25	13.95	9.28	32.5
FTSE100	United Kingdom	2.22	3.56	30	3.25	3.83	18	12.12	9.91	33
MERV	Argentina	6.84	6.53	31	6.42	4.82	26	17.78	8.05	35
IBOVESPA	Brazil	3.67	4.27	29	6.59	5.03	27	16.62	7.81	34
MXX	Mexico	2.60	4.09	22	4.52	5.01	35	13.21	9.82	35.5
TSX	Canada	1.81	3.46	24	3.95	4.91	23	11.58	10.54	33
AMEX	USA	2.03	3.62	23	4.39	4.95	26	12.91	9.91	32.5
NYSE	USA	1.73	3.06	22	4.11	4.71	24	12.37	10.14	32
NASD	USA	2.28	3.66	22	4.74	4.82	25	13.89	9.59	33
SPX500	USA	1.66	3.17	28	3.97	4.97	25	11.83	10.42	32
DJI	USA	1.64	3.20	26	3.64	4.69	24	11.35	10.48	32
AORD	Australia	5.93	7.52	33	2.61	3.77	25	13.39	11.26	35

3.1. The deviation analysis for NTE and CBEDETE

Through the methods described above, we calculated the transfer entropy using TTE, NTE, and CBEDETE methods in different bins and lengths. In Fig. 5, the horizontal axis displays the theoretical transfer entropy, and the vertical axis represents the differences between NTE and TTE (instead by black lines), and those between CBEDETE and TTE (shown by red lines). The dct_{α}^{M} is apparently lower than dnt_{m} at almost all TE values. Meanwhile, with the length increasing, dct_{α}^{M} and dnt_{α}^{M} are both low enough. That is, the deviation becomes extremely small when the sequence length is long enough. For example, in Fig. 5(f), when the length equals 300, the largest dct_{α}^{M} and dnt_{α}^{M} are both about $2 * 10^{-3}$.

Figs. 6–8 show the computation accuracy of the TE calculation using the NTE and CBEDE methods in 3-bin, 4-bin and 5-bin conditions respectively. The calculation errors of CBEDETE are all lower than the ones of NTE in 3-bins,4-bins and 5-bins conditions. With the increase of bin number, the error of NTE grows significantly. It can be seen in Fig. 8(a) that the difference (5-bin and 10-length condition) between NTE and TTE is about 0.25 while the difference between CBEDETE and TTE is only about 0.05.

In short, the computation accuracy of TE calculation by NTE deceases with the increase of length and bin numbers. The bin number is a major factor causing the error of TE calculation. However, deviation of the TE calculation using the CBEDETE method is stable and relatively small, showing that the CBEDETE method is robust in the estimation of transfer entropy in both bin and length scales.

3.2. Application in stock market

Based on the finding that the CBEDETE method achieves higher precision than the NTE method, we apply the CBEDETE method in the financial market to create financial networks with the aim of finding the interaction between stocks and detecting early warning signals of financial crises. Because the search for early warning signals needs short sequences

Table 4
Basic statistics of transfer entropy networks of 2-month sliding window.

Abb.	Market	Out-degree			In-degree			Harmonic centrality		
		Mean	SD	Max	Mean	SD	Max	Mean	SD	Max
KOSPI	Korea	8.60	7.73	32	2.41	2.57	18	18.41	9.01	34.50
PSI	Philippine	8.66	7.46	34	2.15	2.28	18	18.06	8.75	35.50
JKSE	Indonesia	5.96	5.75	29	2.77	2.84	15	16.92	8.22	34.00
STI	Singapore	4.52	5.43	25	2.28	2.78	16	14.50	9.76	32.00
Sensex30	India	4.61	5.02	27	2.83	2.92	19	16.06	8.31	33.00
FKLI	Malaysia	2.25	4.05	23	1.32	2.95	19	8.94	10.08	30.50
TA100	Israel	3.94	5.25	33	4.84	5.59	34	16.14	9.87	35.50
Nikkei225	Japan	5.35	5.14	25	2.46	2.46	18	17.21	6.77	31.50
TWII	Taiwan, China	2.31	3.40	24	2.30	2.80	20	14.08	7.73	31.00
HIS	Hong Kong, China	3.45	4.02	19	2.74	2.77	21	16.41	6.45	28.33
HSCEI	Hong Kong, China	3.71	3.76	21	3.11	2.52	15	17.27	5.14	28.50
CSI 300	China mainland	1.98	2.96	20	2.68	2.39	19	15.11	6.41	28.33
SZI	China mainland	1.96	2.62	20	2.99	2.61	22	15.62	5.56	29.00
SSE180	China mainland	1.83	2.82	20	2.53	2.37	19	14.65	6.66	28.50
SHI	China mainland	1.75	2.59	18	2.40	2.31	18	14.38	6.78	30.00
RTS	Russia	12.20	6.95	33	3.53	2.90	17	21.70	6.31	34.00
NZ50	New Zealand	3.29	5.90	31	0.83	1.75	15	8.78	10.48	33.00
SSMI	Switzerland	2.77	3.66	24	3.05	3.18	17	14.91	8.58	30.50
OMXSPI	Sweden	2.65	3.25	25	3.53	3.17	21	15.91	7.71	29.00
OSEAX	Norway	3.00	3.55	25	3.37	3.08	22	16.31	6.88	31.00
AEX	Netherlands	2.64	3.23	21	3.63	2.96	19	16.25	7.28	27.50
BFX	Belgium	2.01	2.75	17	3.61	3.38	24	14.95	8.26	28.33
ATX	Austria	3.12	3.27	18	3.89	3.31	19	16.75	6.98	29.00
MIB	Italy	2.60	3.09	23	4.15	3.03	18	17.13	5.92	27.33
SMSI	Spain	2.52	2.93	20	3.75	3.11	18	16.39	6.61	28.00
DAX	Germany	1.92	2.34	17	3.95	3.41	22	16.39	6.34	29.00
CAC40	France	2.25	2.71	16	3.60	3.03	23	16.06	6.98	28.50
FTSE100	United Kingdom	1.83	2.60	21	3.06	2.95	16	14.56	7.98	29.00
MERV	Argentina	5.43	4.83	25	5.23	3.38	22	19.55	4.86	30.33
IBOVESPA	Brazil	2.32	2.93	16	5.94	3.99	25	18.25	5.17	31.00
MXX	Mexico	1.75	2.66	15	4.55	4.25	27	15.76	7.59	31.50
TSX	Canada	1.26	2.20	22	4.15	4.17	21	14.02	9.13	29.50
AMEX	USA	1.39	2.51	18	4.48	4.05	22	15.59	7.66	29.00
NYSE	USA	1.11	1.92	17	4.35	4.11	24	15.00	8.19	27.83
NASD	USA	1.53	2.41	15	4.69	3.84	24	16.65	6.58	28.00
SPX500	USA	1.10	1.90	17	4.14	4.42	24	14.31	8.78	29.50
DJI	USA	1.18	2.01	13	3.73	3.94	20	13.74	8.98	27.33
AORD	Australia	6.45	6.52	31	2.16	2.84	18	16.30	9.42	33.00

for its accuracy, our CBEDETE method is just brought to resolve the problem. In order to create stock networks, we first select 38 important stock markets from 4 continents including Asia (15 stocks), Europe (13 stocks), America (9 stocks) and Oceania (1 stock). The detailed contents of stocks are shown in Table 2 [33].

The daily indices are considered and the time duration covers about 15 years from January 1st 2005 to October 25th 2019. The length of the closing price is 4603. For each index, denoted with $\{P_1, P_2, P_3, \ldots, P_t\}$, we analyze the daily log-returns of the closing prices, defined as

$$R_t = ln(P_t) - ln(P_{t-1}), \tag{24}$$

In order to translate the daily log-returns into data format used in the calculation of CBEDETE, we define $R_t = 0$ when $R_t < Q_t(R_t, 0.1)$, where Q_t is a quantile function and let $R_t = 1$ when $R_t \geq Q_t(R_t, 0.1)$. Then the data were split into 2 bins. We set 20 days (about 1-month data), 40 days (about 2-month data) and 60 days (about 3-month data) as the time scales because the sensitivity of short time series is higher than long series. In addition, by employing short time scales as successive segments, we can get more segments than long sequences, which is beneficial for forecasting. We use the 1-day moving step to get more information from successive time scales. Then we calculate the transfer entropy by CBEDETE among 38 stocks by successive time scales, and set the mean value of each transfer matrix as the criterion. When the transfer entropy between two sequences is above this standard, the two nodes representing two series are defined to be connected. The successive networks are built according to this rule. The out-/in-degree and harmonic centralities of the networks in 1-, 2- and 3-month sliding window are shown in Tables 3, 4, and 5. The quantity of stocks, whose out-degrees are above 5, decrease with the increase of the window length shown in Tables 3, 4, and 5 (8 stocks are on the condition of 1-month sliding window, 7 and 6 stocks correspond to 2-month and 3-month window respectively). More specifically, the out-degree of Asian stocks (KOSPI, PSI, Sensex30, NIKKE and JKSE), Oceania stock (AORD), European stock (RTS) and South American stock (MERV) are all above 5 when the length of the sliding window is 1 month. But when the window length is 3 months, the out-degree of MERV and Sensex30 decrease to 3.95 and 3.88 respectively and the out-degree of

Table 5
Basic statistics of transfer entropy networks of 3-month sliding window.

Abb.	Market	Out-degree			In-degree			Harmonic centrality		
		Mean	SD	Max	Mean	SD	Max	Mean	SD	Max
KOSPI	Korea	9.32	7.28	32	2.02	2.15	14	19.84	7.51	34.33
PSI	Philippine	8.67	7.15	30	1.63	1.62	11	19.04	7.36	33.50
JKSE	Indonesia	5.47	5.00	28	2.35	2.41	15	17.59	6.58	32.50
STI	Singapore	4.03	4.40	21	2.02	2.35	13	15.19	8.43	28.83
Sensex30	India	3.88	4.14	21	2.20	2.22	16	16.25	6.94	29.33
FKLI	Malaysia	2.10	3.37	22	1.18	2.79	19	9.88	9.36	28.00
TA100	Israel	3.48	4.56	31	4.70	5.04	34	16.90	8.74	35.50
Nikkei225	Japan	5.27	4.98	23	1.73	1.77	13	17.33	6.06	31.00
TWII	Taiwan, China	1.89	2.99	20	1.90	2.48	17	14.05	6.68	29.00
HIS	Hong Kong, China	3.04	3.62	19	2.01	2.21	18	16.12	5.43	27.33
HSCEI	Hong Kong, China	3.05	3.26	16	2.21	2.02	14	16.33	5.01	26.50
CSI 300	China mainland	1.45	2.44	19	1.78	1.56	12	13.98	6.28	26.33
SZI	China mainland	1.28	1.95	14	2.05	1.86	20	14.23	5.66	26.17
SSE180	China mainland	1.34	2.31	19	1.69	1.59	12	13.78	6.19	26.67
SHI	China mainland	1.22	2.07	16	1.53	1.56	12	12.94	6.79	26.50
RTS	Russia	12.22	5.84	31	2.59	2.23	14	22.54	4.40	32.50
NZ50	New Zealand	3.41	5.76	26	0.69	1.41	12	9.63	10.10	31.00
SSMI	Switzerland	2.12	2.70	18	2.91	2.71	17	15.73	6.88	28.00
OMXSPI	Sweden	1.96	2.34	15	3.22	2.60	16	16.41	5.91	27.33
OSEAX	Norway	2.19	2.78	19	2.88	2.37	15	16.33	5.54	27.50
AEX	Netherlands	2.18	2.55	18	3.33	2.52	14	16.98	5.29	26.00
BFX	Belgium	1.52	2.09	13	3.42	2.89	21	15.87	6.59	28.00
ATX	Austria	2.26	2.51	14	3.40	2.86	17	16.92	5.49	27.00
MIB	Italy	1.81	2.47	18	3.59	2.41	16	17.22	4.37	26.17
SMSI	Spain	1.84	2.30	15	3.11	2.52	13	16.41	5.33	25.50
DAX	Germany	1.46	1.82	10	3.42	2.84	21	16.78	4.36	28.67
CAC40	France	1.68	2.03	13	3.05	2.36	16	16.25	5.53	26.83
FTSE100	United Kingdom	1.48	2.12	17	2.86	2.57	13	15.45	6.18	26.33
MERV	Argentina	3.95	3.87	21	4.32	2.78	21	19.14	3.33	28.50
IBOVESPA	Brazil	1.60	2.33	15	5.08	3.46	19	17.94	4.40	27.33
MXX	Mexico	1.23	2.09	14	4.31	3.81	22	16.18	6.44	28.50
TSX	Canada	0.95	1.70	16	4.00	3.64	17	14.97	7.78	26.67
AMEX	USA	1.02	2.03	15	4.31	3.64	19	16.43	5.88	27.17
NYSE	USA	0.74	1.36	9	4.42	3.77	24	16.01	6.56	27.50
NASD	USA	1.10	1.93	14	4.41	3.53	24	16.97	5.21	27.50
SPX500	USA	0.74	1.37	12	4.27	4.16	24	15.24	7.53	27.50
DJI	USA	0.79	1.55	12	3.68	3.45	18	14.73	7.47	26.17
AORD	Australia	6.33	6.00	30	1.76	2.09	14	17.23	7.85	32.50

RTS rises to 12.22. It means that the distribution of large out-degree nodes are more concentrated with the rise of the sliding widow length.

According to the in-degree distribution of stocks in 1-, 2- and 3-month window, the two stocks (MERV, IBOVESPA) with the largest average in-degree (above 5) belong to South America. The in-degree of US stocks (AMEX, NTSE, and NASD) are equally close to 5.

In order to consider the unconnected vertex, we also calculate the Harmonic centrality following Boldi and Vigna [34]:

$$Har(u) = \sum_{d(u,v)<\infty, u\neq v} \frac{1}{d(u,v)} \tag{25}$$

where $d(u, v)$ is the shortest-path distance between the node u and the node v. The Harmonic centralities of stocks which indicate the uniform distribution of market centrality increase with the length of the sliding window (Harmonic centrality of RTS in one month is 18.54, two months 21.69, and three months 22.54). That is, the network which is created by the longer window often yields more information. To be specific, only 2 Harmonic centralities of stocks (RTS and MERV) are above 17 when the length is 1 month. But when the length of the stocks increase to 3 months, about 9 centralities of stocks among Asian (KOSP, PSI, JKSE, Nikkei225), European (RTS, MIB), South American (MERV, IBOVESPA), Oceania (AROD) are above 17.

For more information of evolution of stock network, we extract the highest out-degree and in-degree from each sliding widow of 1, 2 and 3 month(s) shown in Figs. 9 and 10. The stocks whose out-degree and in-degree are the biggest correspond to the most influential markets and most influenced markets respectively. The most influential markets in Fig. 9(c) are frequently RTS, KOSPI, PSI, AORD and NIKKE whose closing times are before those of America markets. Similarly, the most influenced markets in Fig. 10(c) are frequently IBOVESPA, NYSE NASD and MERV whose closing times are after those of Asian and European markets. These results further confirm the temporal proximity effects [35,36]. In

Table 6
The indicator result of financial crisis.

Crisis ID	Peak ID	Crisis description	The half-month window		
			Crisis date	Indicator date	Advance days
C1	Pe2	The Global financial crisis	2008/9/14	2006/6/5	832
C2	Pe3	The worlds three largest rating firms downgraded the Greeces sovereign rating	2009/12/8	2008/10/31	403
C3	Pe4	Japanese financial crisis	2012/5/1	2011/8/30	245
C4	NO signal	Chinese Financial Industry "Money Shortage"	2013/6/19	N/A	N/A
C5	Pe5	China's stock market crash	2015/6/19	2013/7/11	708
C6	Pe6	The biggest one-day point drops in the Dow's history	2018/2/15	2015/11/4	834
Crisis ID	Peak ID	Crisis description	The 1-month window		
			Crisis date	Indicator date	Advance days
C1	Pe2	The Global financial crisis	2008/9/14	2006/6/4	833
C2	Pe3	The worlds three largest rating firms downgraded the Greeces sovereign rating	2009/12/8	2008/11/11	392
C3	Pe4	Japanese financial crisis	2012/5/1	2011/8/14	261
C4	NO signal	Chinese Financial Industry "Money Shortage"	2013/6/19	N/A	N/A
C5	Pe5	China's stock market crash	2015/6/19	2013/7/21	698
C6	Pe6	The biggest one-day point drops in the Dow's history	2018/2/15	2015/11/15	823
Crisis ID	Peak ID	Crisis description	The 2-month window		
			Crisis date	Indicator date	Advance days
C1	Pe3	The Global financial crisis	2008/9/14	2007/8/12	399
C2	Pe4	The worlds three largest rating firms downgraded the Greeces sovereign rating	2009/12/8	2008/12/1	372
C3	Pe5	Japanese financial crisis	2012/5/1	2011/8/14	261
C4	Pe6	Chinese Financial Industry "Money Shortage"	2013/6/19	2013/5/19	31
C5	Pe7	China's stock market crash	2015/6/19	2014/11/14	217
C6	Pe8	The biggest one-day point drops in the Dow's history	2018/2/15	2015/12/22	786
Crisis ID	Peak ID	Crisis description	The 3-month window		
			Crisis date	Indicator date	Advance days
C1	Pe2	The Global financial crisis	2008/9/14	2007/9/3	377
C2	Pe3	The worlds three largest rating firms downgraded the Greeces sovereign rating	2009/12/8	2008/12/22	351
C3	Pe4	Japanese financial crisis	2012/5/1	2011/9/8	236
C4	Pe5	Chinese Financial Industry "Money Shortage"	2013/6/19	2013/6/14	5
C5	Pe6	China's stock market crash	2015/6/19	2014/12/10	191
C6	Pe7	The biggest one-day point drops in the Dow's history	2018/2/15	2016/1/12	765

Fig. 9(f), the least influential markets are frequently FKLI, STI and Sensex30 which all belong to the Asian plate. The least influenced markets in Fig. 10(f) are frequently RTS, KOSPI, PSI and FKLI, which means the out-degree and in-degree of the same stock are usually inversely related. This conclusion is the same as Vrost et al. [35,36].

To specify this statement, we calculate the distribution of average in/out-degree of 1-, 2- and 3-month length shown in Fig. 12. The inverse proportional relation becomes increasingly obvious with the increase of the window length (2-month and 3-month). But in 1-month condition, the relation appears to be a weak positive correlation. This anomaly may be attributed to the noise effect caused by the short window.

From Fig. 9(a) to (c), the most influential markets become more concentrated. In Fig. 9(a), most of the stocks are defined as most influential markets but few stocks are the most influential markets in Fig. 9(c). Compared with Fig. 9(c), the extra stocks in Fig. 9(a), which are still assessed as the most influential markets, could be seen as noise. But we can also get more information from the "noise" in short length windows. Take for example the small parts of Figs. 9(a) and 10(a) (between January 1st in 2008 and January 1st in 2009), we extract the separate paragraph in Fig. 11. The whole month of the 2008 financial crisis is shown by the blue dotted box. In Fig. 11(a), the most influential markets during the 2008 financial crisis are HIS, ATX, SSMI, AORD, Sensex30, STI, JKSE, PSI and RTS. In Fig. 11(b), the most influenced markets during the 2008 financial crisis are HSCEI, NASD, AMEX, TSX, Sensex30, STI, JKSE and KOSPI.

Based on the analysis of the influence effect of the financial crisis, we calculate the ratio of link to all possible links for each successive stock network. In Fig. 13, the gray line symbolizes the ratio of network links of four time scales (half, one, two and three month(s)). The red curve represents the result of gray line polished by Fast-Fourier transformation (FFT) [37]. The red and blue vertical lines indicate the peaks of the smoothed curve and the crisis events respectively.

Prior to each crisis event (C1. The global financial crisis on September 14, 2008, C2. The worlds three largest Rating firms downgraded the Greeces sovereign rating on December 8, 2009, C3. Japanese financial crisis May 1, 2012, C4. Chinese Financial Industry Money Shortage on June 19, 2013, C5. China's stock market crash on June 19, 2015, C6. The biggest one-day point drops in the Dow's history on February 5, 2018.) one can find a corresponding peak as an early warning signal. The peaks marked by gray and red fonts represent the false signals and true signals respectively.

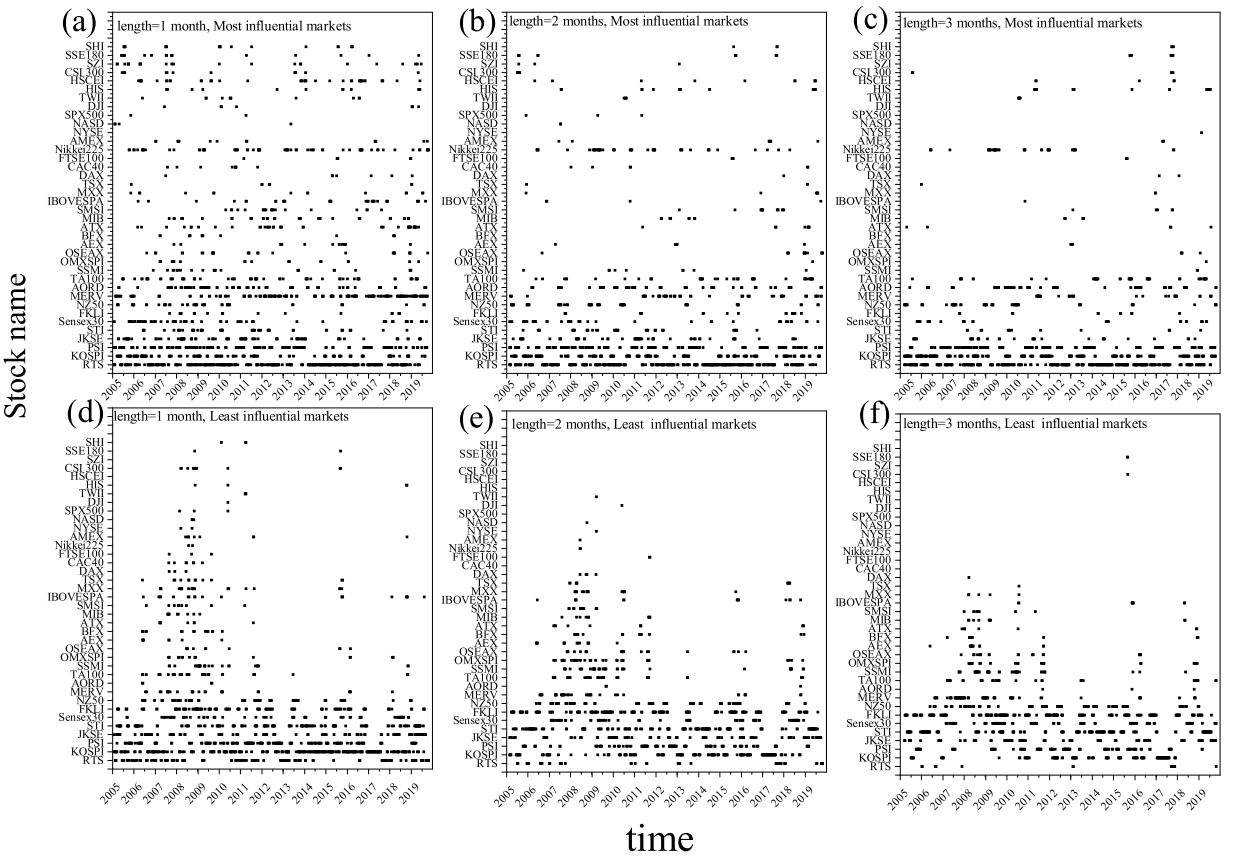

Fig. 9. The evolution of the most influential and the least influential markets. (a), (b) and (c) illustrate the evolution of the most influential (the highest out-degree) markets whose window sizes are 1, 2 and 3 month(s) respectively. (d), (e) and (f) indicate the evolution of the least influential (the lowest out-degree) markets whose window sizes are 1, 2 and 3 month(s) respectively..

Table 7
The statistics of effective peaks.

	The half-month window	The 1-month window	The 2-month window	The 3-month window
Total number of peaks	7	7	9	8
Effective peaks	5	5	6	6
Invalid peaks	2	2	3	2

Due to short window lengths of the link number, some invalid positive signs of crises arise such as the Pe1 in Fig. 13(a). There also exist some exceptions that no signals appear prior to the crisis such as C4 in the Fig. 13(a) and (b). With increases of the window length, the noise of the false peak begins to decrease and true positive signs of crises become clearer as seen in the Fig. 13(d). One can understand this result from the viewpoint of globalization: when the global financial system works perfectly, financial markets distributed in the world have a preference for globalization, which can make the system works efficiently. But a high degree of globalization (highly relevant markets) also means a high systematic risk, namely, shocks in a special market can spread easily and quickly to markets all over the world, which may lead to a global crisis. When a specific incident occurs, institutions being aware of the risks will take actions to filter out the shocks, and the ratio of links will decrease. The crisis time herein is determined by occurrence of a representative incident, while the initial shock occurs occasionally before the crisis time. Consequently, there exists a several-month delay for each crisis, and the crises occur at weakly linked states (less information exchange).

The specific results of the early warning of the financial crisis [16,18–21,38–44] are shown in Tables 6 and 7. In Table 7, the effective peaks increase with the rise of the window length, such as 5 effective peaks in the case of the 1-month window but 6 effective peaks when the window is 3 months.

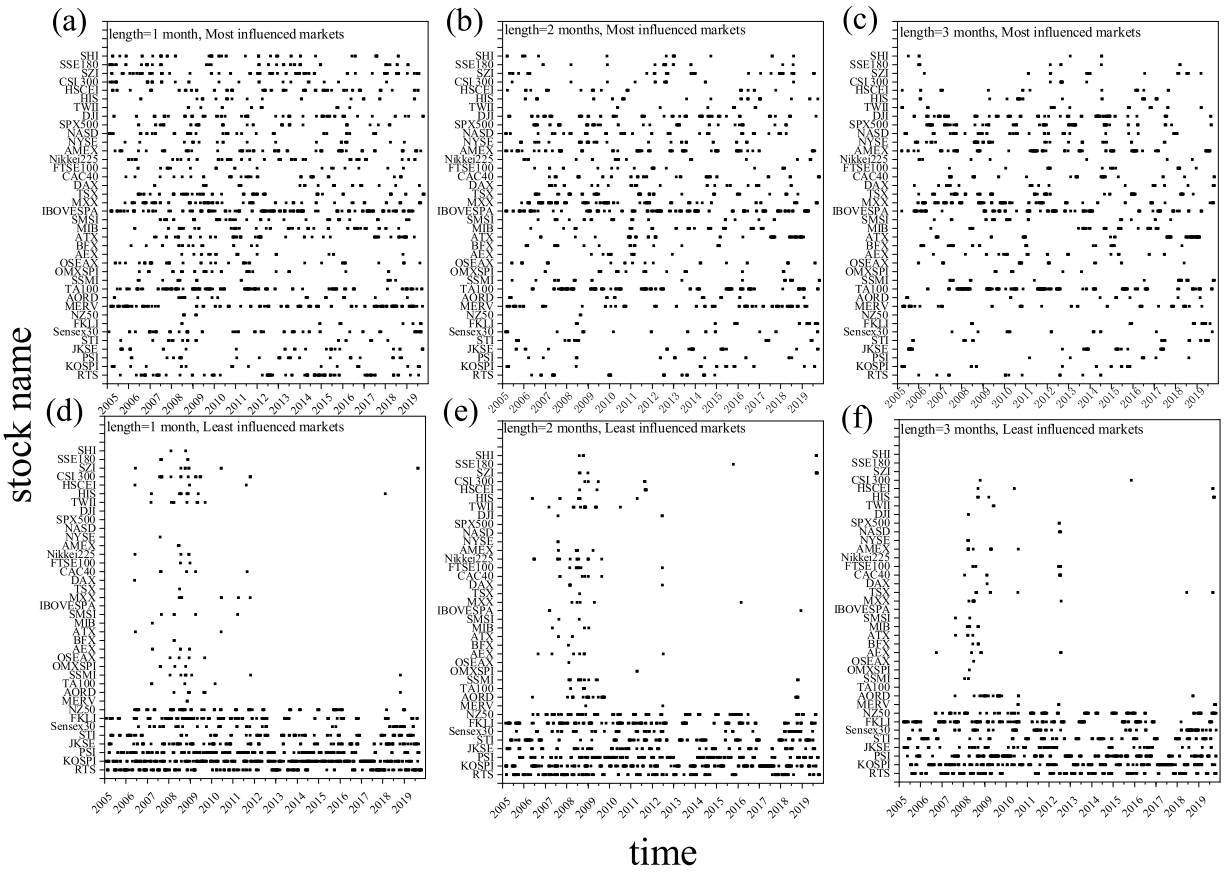

Fig. 10. The evolution of the most influenced and the least influenced markets. (a), (b) and (c) illustrate the evolution of the most influenced (the highest in-degree) markets whose window sizes are 1, 2 and 3 month(s) respectively. (d), (e) and (f) indicate the evolution of the least influenced (the lowest in-degree) markets whose window sizes are 1, 2 and 3 month(s) respectively.

4. Conclusion and discussion

Focusing on the needs of short sequences as indicators of financial crisis and the deviation of the transfer entropy calculation of short sequence, we propose a method named CBEDETE to reduce the bias of transfer entropy of short financial series.

We compare the accuracy between the CBEDETE method and the NTE method in TE calculation for short sequences. The results show that the bias of TE by the CBEDETE method is reduced compared with the NTE method in all length and bin conditions. We further explore that the TE calculation bias of NTE caused by bin conditions is larger than that caused by length. After confirming the accuracy of CBEDETE, we use the CBEDETE to estimate the transfer entropy between 38 important world stocks. By applying the sliding window technique over short sequences and the threshold criterion (above the mean value of each sliding transfer entropy matrix), we create directed financial networks for each window and make an analysis of the influential/influenced effect of stocks. Through the evolution of out-/in-degree of stock network, we verify the temporal proximity effects that Asian stocks, Oceanian stocks and European stocks often have more influential effect but American stocks have more influenced effect because of the closing times. Finally, we monitor the dynamic evolution of the ratio of network links and extract Fourier-smoothed for the sequence of dynamic ratio curve. We find that the effective peaks of the smoothed line appear before the corresponding extreme events, especially the global financial crisis in 2008.

Our results not only show the validity of the CBEDETE method in short sequences, but also reveal the individual stocks affected by financial crises and early warning signals of financial crises. By monitoring vulnerable stocks by financial crises and the effective peaks of link ratio curve of stock networks, our method intends to inform government efforts to prevent financial risks.

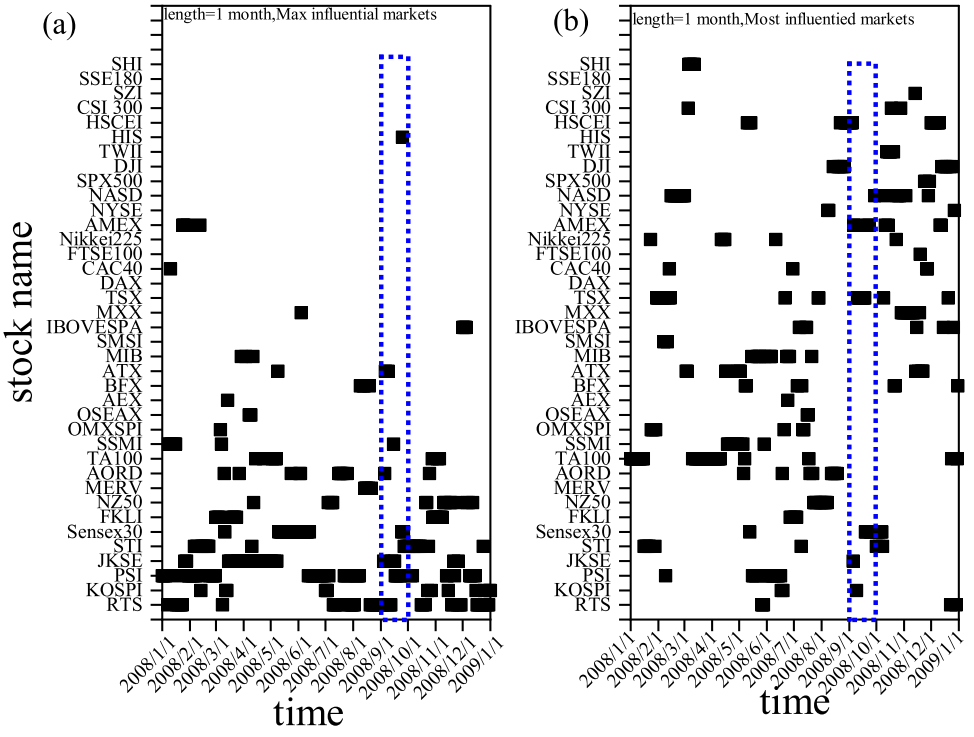

Fig. 11. The most influential and influenced markets during the 2008 global financial crisis. (a) The most influential markets between September 1st and October 1st. (b) The most influenced markets between September 1st and October 1st.

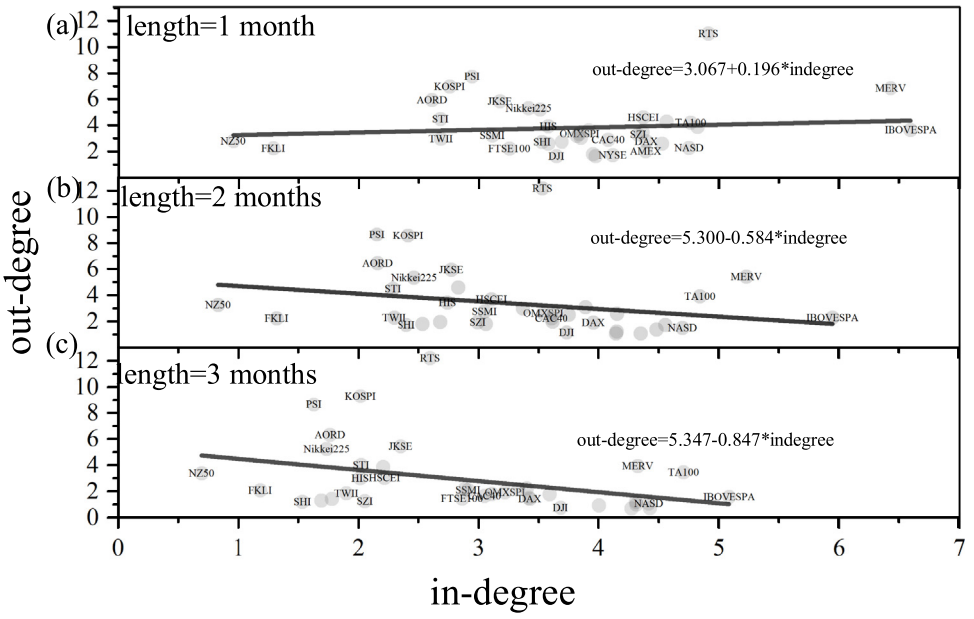

Fig. 12. The average in/out-degree of stock networks. (a), (b) and (c) indicate the distribution of the average in/out-degree of stock networks whose window size is 1, 2 and 3 month(s) respectively.

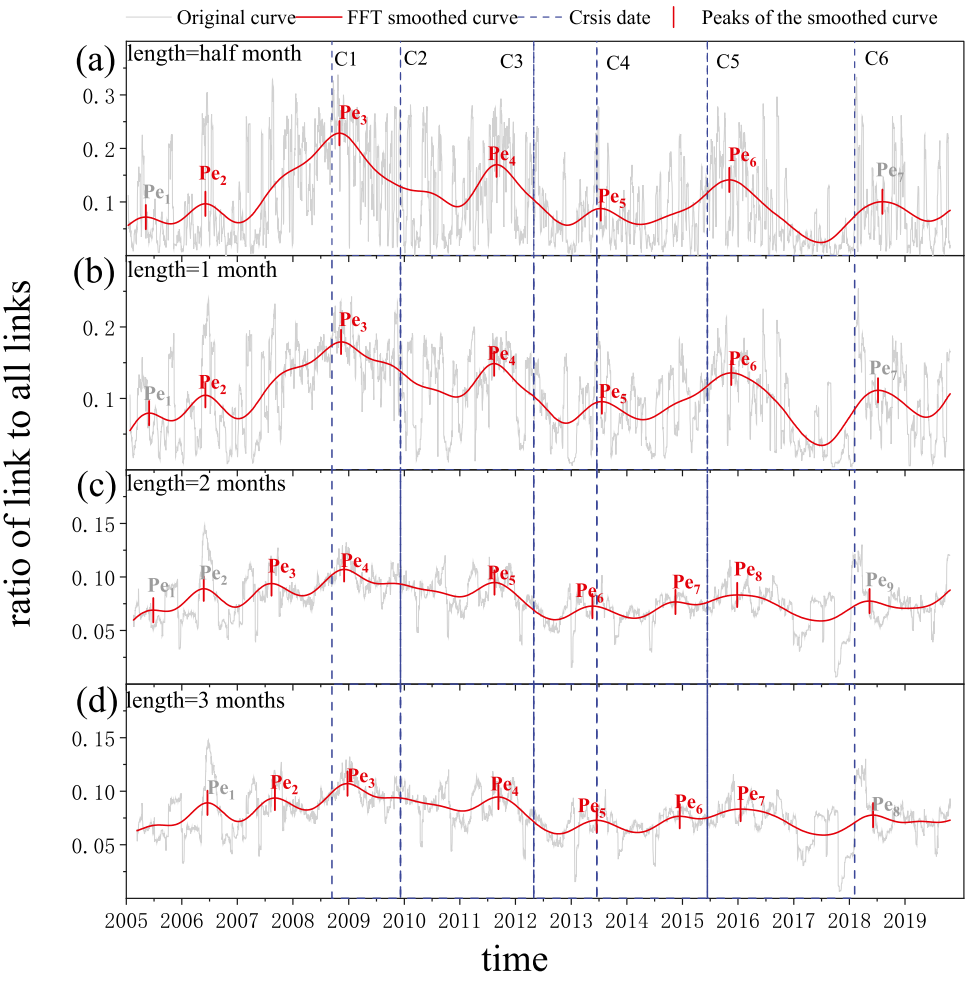

Fig. 13. Indicator of financial crisis. (a), (b), (c) and (d) illustrate the evolution of network links with half-, 1-, 2- and 3-month sliding windows respectively. The gray line indicates the ratio of link to all possible links created by the CBEDETE method. The red curve represents the smoothed result of the gray line whose peaks are shown by red vertical line. From C1 to C6 are the financial crisis events: C1. The global financial crisis on September 14, 2008, C2. The world's three largest Rating firms downgraded the Greece's sovereign rating on December 8, 2009, C3. Japanese financial crisis May 1, 2012, C4. Chinese Financial Industry "Money Shortage" on June 19, 2013, C5. China's stock market crash on June 19, 2015, C6. The biggest one-day point drops in the Dow's history on February 5, 2018.

CRediT authorship contribution statement

Lu Qiu: Designed the research, Performed the calculation, Analyzed the data, Wrote the paper, Manuscript revision. **Huijie Yang:** Designed the research, Performed the calculation, Manuscript revision.

Declaration of competing interest

The authors declare that they have no known competing financial interests or personal relationships that could have appeared to influence the work reported in this paper.

Acknowledgments

The work is supported by The Youth Project of Humanities and Social Sciences Financed by Ministry of Education under Grant No. 18YJC910010 (L. Qiu). Research Projects of Humanities and Social Sciences of Shanghai Normal University under Grant No. A-7031-18-004023 (L. Qiu). Lu Qiu and Huijie Yang designed the research performed the calculation. Lu Qiu analyzed the data and wrote the paper. The authors contributed to manuscript revision, read and approved the submitted version.

The authors read and approved the submitted version.

References

[1] S. Battiston, J.D. Farmer, A. Flache, D. Garlaschelli, A.G. Haldane, H. Heesterbeek, C. Hommes, C. Jaeger, R. May, M. Scheffer, Complexity theory and financial regulation, Science 351 (2016) 818–819, http://dx.doi.org/10.1126/science.aad0299.

[2] W. Zhong, H. An, X. Gao, X. Sun, The evolution of communities in the international oil trade network, Physica A 413 (2014) 42–52, http://dx.doi.org/10.1016/j.physa.2014.06.055.

[3] D. Covitz, N. Liang, G.A. Suarez, The evolution of a financial crisis: Collapse of the asset-backed Commercial Paper Market, J. Finance 68 (2013) 815–848, http://dx.doi.org/10.1111/jofi.12023.

[4] F. Moshirian, The global financial crisis and the evolution of markets, institutions and regulation, J. Bank. Financ. 35 (2011) 502–511, http://dx.doi.org/10.1016/j.jbankfin.2010.08.010.

[5] T.C. Silva, S.R.S. De Souza, B.M. Tabak, Structure and dynamics of the global financial network, Chaos Solitons Fractals 88 (2016) 218–234, http://dx.doi.org/10.1016/j.chaos.2016.01.023.

[6] L. Sandoval, I.D.P. Franca, Correlation of financial markets in times of crisis, Physica A 391 (2012) 187–208, http://dx.doi.org/10.1016/j.physa.2011.07.023.

[7] G. Sugihara, R. May, H. Ye, C.H. Hsieh, E. Deyle, M. Fogarty, S. Munch, Detecting causality in complex ecosystems, Science 338 (2012) 496–500, http://dx.doi.org/10.1126/science.1227079.

[8] C. Brunetti, J.H. Harris, S. Mankad, G. Michailidis, Interconnectedness in the interbank market, J. Financ. Econ. 133 (2019) 520–538, http://dx.doi.org/10.1016/j.jfineco.2019.02.006.

[9] P. Fiedor, Networks in financial markets based on the mutual information rate, Phys. Rev. E 052801 (2014) 1–7, http://dx.doi.org/10.1103/PhysRevE.89.052801.

[10] K. Lim, S. Kim, S.Y. Kim, Information transfer across intra/inter-structure of CDS and stock markets, Physica A 486 (2017) 118–126, http://dx.doi.org/10.1016/j.physa.2017.05.084.

[11] P. Yang, P. Shang, A. Lin, Financial time series analysis based on effective phase transfer entropy, Physica A 468 (2017) 398–408, http://dx.doi.org/10.1016/j.physa.2016.10.085.

[12] L. Sandoval, Structure of a global network of financial companies based on Transfer Entropy, Entropy 16 (2014) 4443–4482, http://dx.doi.org/10.3390/e16084443.

[13] O. Kwon, J.S. Yang, Information flow between stock indices, Epl. 82 (2008) http://dx.doi.org/10.1209/0295-5075/82/68003.

[14] J. He, P. Shang, H. Xiong, Multidimensional scaling analysis of financial time series based on modified cross-sample entropy methods, Physica A 500 (2018) 210–221, http://dx.doi.org/10.1016/j.physa.2018.02.105.

[15] X. Mao, P. Shang, Transfer entropy between multivariate time series, Commun. Nonlinear Sci. Numer. Simul. 47 (2017) 338–347, http://dx.doi.org/10.1016/j.cnsns.2016.12.008.

[16] L. Zhou, L. Qiu, C. Gu, H. Yang, Immediate causality network of stock markets, Epl 121 (2018) 48002, http://dx.doi.org/10.1209/0295-5075/121/48002.

[17] M. Gutiérrez-roig, J. Borge-holthoefer, A. Arenas, J. Perelló, Mapping individual behavior in financial markets : synchronization and anticipation, EPJ Data Sci. 8 (2019) 1–18, http://dx.doi.org/10.1140/epjds/s13688-019-0188-6.

[18] G. Buccheri, S. Marmi, R.N. Mantegna, Evolution of correlation structure of industrial indices of U.S. equity markets, Phys. Rev. E 88 (2013) 012806, http://dx.doi.org/10.1103/PhysRevE.88.012806.

[19] M.C. Münnix, T. Shimada, R. Schäfer, F. Leyvraz, T.H. Seligman, T. Guhr, H.E. Stanley, Identifying states of a financial market, Sci. Rep. 2 (2012) 00644, http://dx.doi.org/10.1038/srep00644.

[20] L. Qiu, C. Gu, Q. Xiao, H. Yang, G. Wu, State network approach to characteristics of financial crises, Physica A 492 (2018) 1120–1128, http://dx.doi.org/10.1016/j.physa.2017.11.042.

[21] S. Hoon, J. Woo, The network connectedness of volatility spillovers across global futures markets, Physica A 526 (2019) 120756, http://dx.doi.org/10.1016/j.physa.2019.03.121.

[22] M. Scheffer, J. Bascompte, W.A. Brock, V. Brovkin, S.R. Carpenter, V. Dakos, H. Held, E.H. Van Nes, M. Rietkerk, G. Sugihara, Early-warning signals for critical transitions, Nature 461 (2009) 53–59, http://dx.doi.org/10.1038/nature08227.

[23] X. Pan, L. Hou, M. Stephen, H. Yang, C. Zhu, Evaluation of scaling invariance embedded in short time series, PLoS One 9 (2014) 1–27, http://dx.doi.org/10.1371/journal.pone.0116128.

[24] X. Pan, L. Hou, M. Stephen, H. Yang, Long-term memories in online users' selecting activities, Phys. Lett. A 378 (2014) 2591–2596, http://dx.doi.org/10.1016/j.physleta.2014.07.012.

[25] J. Qi, H. Yang, Hurst exponents for short time series, Phys. Rev. E 84 (2011) 066114, http://dx.doi.org/10.1103/PhysRevE.84.066114.

[26] W. Zhang, L. Qiu, Q. Xiao, H. Yang, Q. Zhang, J. Wang, Evaluation of scale invariance in physiological signals by means of balanced estimation of diffusion entropy, Phys. Rev. E 86 (2012) 056107, http://dx.doi.org/10.1103/PhysRevE.86.056107.

[27] N. Scafetta, Fractal and Diffusion Entropy Analysis of Time Series: Theory, concepts, applications and computer codes for studying fractal noises and Lvy walk signals, Aquat. Toxicol. 91 (2009) 151–160.

[28] P. Grigolini, D. Leddon, N. Scafetta, Diffusion entropy and waiting time statistics of hard-x-ray solar flares, Phys. Rev. E 65 (2002) 046203, http://dx.doi.org/10.1103/PhysRevE.65.046203.

[29] N. Scafetta, B.J. West, Solar Flare Intermittency and the Earth's Temperature Anomalies, Phys. Rev. Lett. 90 (2003) 248701, http://dx.doi.org/10.1103/PhysRevLett.90.248701.

[30] H. Yang, F. Zhao, L. Qi, B. Hu, Temporal series analysis approach to spectra of complex networks, Phys. Rev. E 69 (2004) 066104, http://dx.doi.org/10.1103/PhysRevE.69.066104.

[31] N. Scafetta, D. Marchi, B.J. West, Understanding the complexity of human gait dynamics, Chaos 19 (2009) 7–18, http://dx.doi.org/10.1063/1.3143035.

[32] J. Perelló, M. Montero, L. Palatella, I. Simonsen, J. Masoliver, Entropy of the Nordic electricity market: anomalous scaling, spikes, and mean-reversion, J. Stat. Mech. Theory Exp. 2006 (2006) 11011, http://dx.doi.org/10.1088/1742-5468/2006/11/P11011.

[33] https://www.wind.com.cn/NewSite/wft.html.

[34] P. Boldi, S. Vigna, Axioms for centrality, Internet Math. 10 (2014) 222–262, http://dx.doi.org/10.1080/15427951.2013.865686.

[35] T. Vrost, Lyócsa, E. Baumöhl, Granger causality stock market networks: Temporal proximity and preferential attachment, Physica A 427 (2015) 262–276, http://dx.doi.org/10.1016/j.physa.2015.02.017.

[36] E. Baumöhl, E. Koenda, Lyócsa, T. Vrost, Networks of volatility spillovers among stock markets, Physica A 490 (2018) 1555–1574, http://dx.doi.org/10.1016/j.physa.2017.08.123.

[37] Y. Wang, J. Yang, W. Yin, Y. Zhang, A new alternating minimization algorithm for total variation image reconstruction, SIAM J. Imaging Sci. 1 (2008) 248–272, http://dx.doi.org/10.1137/080724265.

[38] F. Ren, W.X. Zhou, Dynamic evolution of cross-correlations in the Chinese stock market, PLoS One 9 (2014) e97711, http://dx.doi.org/10.1371/journal.pone.0097711.

[39] L.P. Samarakoon, Contagion of the eurozone debt crisis, J. Int. Financ. Mark. Inst. Money 49 (2017) 115–128, http://dx.doi.org/10.1016/j.intfin.2017.03.001.
[40] J.W. Lee, A. Nobi, State and network structures of Stock Markets Around the Global Financial Crisis, Comput. Econ. 51 (2018) 1–16, http://dx.doi.org/10.1007/s10614-017-9672-x.
[41] S. Kumar, N. Deo, Correlation and network analysis of global financial indices, Phys. Rev. E 86 (2012) 026101, http://dx.doi.org/10.1103/PhysRevE.86.026101.
[42] J. Wei, J. Wu, J. Fu, The analysis and Countermeasures of Chinese Financial Industry Money Shortage, Ind. Technol. Econ. 5 (2014) 3–13, http://dx.doi.org/10.3969/j.issn.1004-910X.2014.05.001.
[43] Y. Yuan, Y. Qi, An Empirical study on the volatility of the real estate sector and the overall stock market in the shocks of financial crisis and real Estate Regulations, Statist. Res. 36 (2019) 38–49, http://dx.doi.org/10.19343/j.cnki.11-1302/c.2019.02.004.
[44] https://finance.yahoo.com/news/biggest-one-day-point-drops-205600481.html.